Chinese Journal of Aeronautics, (2016), 29(2): 479–491

Chinese Society of Aeronautics and Astronautics
& Beihang University

Chinese Journal of Aeronautics

cja@buaa.edu.cn
www.sciencedirect.com

Relative dynamics estimation of non-cooperative spacecraft with unknown orbit elements and inertial tensor

Yu Han [a,b,*], Zhang Xiujie [c], Liu Lingyu [a], Wang Shuo [b], Song Shenmin [b]

[a] Beijing Institute of Astronautical Systems Engineering, Beijing 100076, China
[b] Center for Control Theory and Guidance Technology, Harbin Institute of Technology, Harbin 150001, China
[c] Academy of Fundamental and Interdisciplinary Science, Harbin Institute of Technology, Harbin 150001, China

Received 27 March 2015; revised 31 August 2015; accepted 27 January 2016
Available online 24 February 2016

KEYWORDS

Cubature Kalman filter;
MAP estimator;
Non-cooperative spacecraft;
Relative motion;
Stereo vision

Abstract The state estimation for relative motion with respect to non-cooperative spacecraft in rendezvous and docking (RVD) is a challenging problem. In this paper, a completely non-cooperative case is considered, which means that both orbit elements and inertial tensor of target spacecraft are unknown. By formulating the equations of relative translational dynamics in the orbital plane of chaser spacecraft, the issue of unknown orbit elements is solved. And for the problem for unknown inertial tensor, we propose a novel robust estimator named interaction cubature Kalman filter (InCKF) to handle it. The novel filter consists of multiple concurrent CKFs interlacing with a maximum a posteriori (MAP) estimator. The initial estimations provided by the multiple CKFs are used in a Bayesian framework to form description of posteriori probability about inertial tensor and the MAP estimator is applied to giving the optimal estimation. By exploiting special property of spherical-radial (SR) rule, a novel method with respect to approximating the likelihood probability of inertial tensor is presented. In addition, the issue about vision sensor's location inconformity with center mass of chaser spacecraft is also considered. The performance of this filter is demonstrated by the estimation problem of RVD at the final phase. And the simulation results show that the performance of InCKF is better than that of extended Kalman filter (EKF) and the estimation accuracy of pose and attitude is relatively high even in the completely non-cooperative case.

1. Introduction

Estimation of relative motion between spacecraft has attracted extensive attention in the last few years.[1] Especially, it is very important in the rendezvous and docking (RVD) research.[2] RVD is a key technology, which is required for many space

* Corresponding author. Tel.: +86 10 68756947.
E-mail address: yuhanihit@163.com (H. Yu).
Peer review under responsibility of Editorial Committee of CJA.

ELSEVIER Production and hosting by Elsevier

http://dx.doi.org/10.1016/j.cja.2016.01.013

missions such as assembly in orbit, re-supply of orbital platforms, repair of spacecraft in orbit, etc.[3] The RVD missions which have been implemented so far include orbital express[4], engineering test satellite (ETS)-VII[5] and automated transfer vehicle (ATV).[6] However, most of them are treated as cooperative space missions. Namely, relative estimation algorithm depends on information exchange between spacecraft or some type of beacon preassembled in target spacecraft.[7,8]

In fact, many RVD missions are involved with non-cooperative spacecraft, such as enemy satellite, major in-orbit satellites, etc. In these missions, the estimation of relative motion turns to be more complicated, as there is a little information about pose and configuration of the target spacecraft. And grappling and anchoring to non-cooperative objects is regarded as the top technical challenge in the demonstration mission of NASA flagship technology.[9] In Ref.[10], non-cooperative spacecraft is defined as, ''non-cooperative spacecraft means that there is no communication system or any other active sensor, and thus its orientation cannot be determined by electronic inquiry or signal emission".

There is little literature that deals with the problem of relative motion estimation about non-cooperative target. Vision-based estimation of relative motion could be a kind of available solutions for the problem of RVD missions at the final phase. Specially, stereovision technique is widely used in the motion estimation.[11–15] In general, the geometrical characteristic of spacecraft is recognized by vision sensors sampling a sequence of images, such as solar panel, antenna boom, payload attach fitting, nozzle of apogee motor. In Ref.[11], it took four natural features placed on the target satellite to determine relative pose in real time. However, its effectiveness for non-cooperative target is limited, as it supposes that the positions of feature points on target satellite are previously known. Xu et al.[12] proposed a method in which solar panel of spacecraft is identified by Hough transform and provided closed-form expressions about position and attitude of spacecraft. More recently, Liu et al.[13] developed a novel algorithm which is based on information fusion of multi-feature to estimate the pose of non-cooperative satellite. And it takes the contour and nozzle of target satellite as the multi-feature. In addition to the above-mentioned feature-based algorithms, there is another way to determine pose information. In Ref.[14], the relative motion was estimated using a distinctive approach which is named algorithm of mode-based pose refinement. Nevertheless, it needs to take advantage of a prior knowledge of target 3D model and its initial pose estimation. Zhou et al.[15] applied extended Kalman filter (EKF) to estimate the relative states. However, it is not referred to the situation that vision sensor's location does not coincide with the spacecraft's center of mass (c. m.). If the above situation is concerned, a novel kinematic coupling between the rotation and translation will exist.[16] And considerable errors in a rendezvous problem will take place if this perturbation is ignored.

The equations of translational relative dynamics between spacecraft are always resolved in the frame of target spacecraft (e. g., Clohessy–Wiltshire (C–W) equations). However, it is not suitable for non-cooperative applications since the orbit elements of target spacecraft are unknown. In addition, the inertial tensor of target spacecraft is also unknown. The main purpose of this paper is to design a robust filtering scheme for estimating relative motion status with respect to non-cooperative scenarios that both orbit elements and inertial tensor of target spacecraft are unknown. And the issue about unknown inertial tensor is the major consideration in this paper. Actually, this issue can be regarded as a combined estimation problem. In other words, it means that both state variables of system and unknown inertia tensor are estimated simultaneously at the given observations. One approach for combined estimation is to take the scale of unknown inertia tensor as state augmentation.[17,18] However, it just takes the principal moments of inertia into account and does not directly give the value of inertial tensor. Besides, the increase of dimension of the state vector is likely to cause the estimation inconsistency particularly in the nonlinear dynamic system. Another approach is to design an interactive filter, which is either to estimate the state from the unknown parameters or to estimate the unknown parameters from state.[19] Nevertheless, the scheme in Ref.[19] is open-loop and it takes iterated extended Kalman filter (IEKF) which is of low precision and inconsistency for a high-dimensional nonlinear system to estimate state. In this paper, we take the same idea to deal with the problem of the unknown inertia tensor by designing an external estimator interlaced with cubature Kalman filter (CKF). It is proved that CKF is optimal when embedded in the Bayesian filter and its precision and consistency with respect to a high-dimensional nonlinear system are better than those of conventional nonlinear filters,[20] such as EKF, unscented Kalman filter, quadrature Kalman filter, etc. Furthermore, we propose a novel method to estimate the probability density of inertia tensor. As for the issue about the unknown orbit elements of target spacecraft, we take equations resolved in the frame of chaser spacecraft to describe the translational relative dynamics between spacecraft. And the case that vision sensor's location does not coincide with chaser spacecraft's c. m. is also considered.

The rest of this paper is organized as follows: Section 2 presents the model of relative dynamics; Section 3 states the problem of RVD for non-cooperative target; Section 4 presents the algorithm of InCKF; Section 5 gives the numerical simulation results and demonstrates the performance of InCKF for pose estimation; Conclusion remarks are drawn in Section 6.

2. Mathematical formulation

Presuppose that two spacecraft are in orbit around the earth. One is the chaser spacecraft with respect to a reference satellite on an eccentric orbit and the other is the target spacecraft in a circular orbit. It is assumed that the chaser spacecraft is equipped with two cameras to capture images of N feature points on the target spacecraft. And the positions of feature points on the target spacecraft are unknown. The relative orbital motion of the two spacecrafts is illustrated in Fig. 1.

In Fig. 1, the following coordinate systems are concerned: F_I, the Earth-centered inertial reference frame, whose original O_I is located in the center of the Earth, with the fact that its X_I is pointed to the vernal equinox, its Z_I is directed along the rotational axis of the Earth, and Y_I complies with the right-handed rule; F_C, a local-vertical and local-horizontal Cartesian reference frame fastened to the chaser spacecraft c. m., with X_C being a unit vector directed from the center of the Earth to c. m., Z_C towards the direction of chaser spacecraft motion in the chaser's orbital plane, and Y_C completing the dextral triad; F_T, a Cartesian right-hand body-fixed reference frame with its

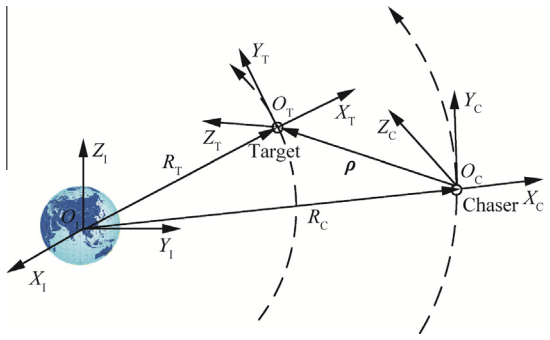

Fig. 1 Relative motion of chaser and target.

original O_T riveting to the target spacecraft's c. m. In the following article, we premise that the orbital reference frame F_C accords with the body-fixed frame of the chaser spacecraft. R_T and R_C are the distance from the target and chaser to the Earth, respectively. And the vector between the c. m. of chaser and target, resolved in F_C, is denoted by $\boldsymbol{\rho} = [x, y, z]^T$.

2.1. Relative translational dynamics

It is considered that the target spacecraft is non-cooperative and the orbit angular velocity of the target spacecraft is unknown. So the conservative relative translational dynamics which projects onto the orbital plane of target spacecraft is invalid. Thus, we formulate equations in the orbital plane of chaser spacecraft to present the relative motion at the final phase of rendezvous and docking as

$$\begin{cases} \ddot{x} + 2n_y\dot{z} - n_y^2 x + \dot{n}_y z = \frac{2ux}{R_C^3} - f_x \\ \ddot{y} = -\frac{uy}{R_C^3} - f_y \\ \ddot{z} - 2n_y\dot{x} - n_y^2 z - \dot{n}_y x = -\frac{uz}{R_C^3} - f_z \end{cases} \tag{1}$$

where $\boldsymbol{f} = [f_x, f_y, f_z]^T$ is the force of the chaser spacecraft in unit mass; u is the gravitational constant; $\boldsymbol{n} = [0, n_y, 0]^T$ is the orbit angular velocity of the chaser spacecraft, resolved in F_C, and $n_y = \dot{\theta}_C$, $\dot{n}_y = \ddot{\theta}_C$; distance R_C is given as

$$R_C = \frac{a_C(1 - e_C^2)}{(1 + e_C \cos\theta_C)} \tag{2}$$

And θ_C is the true anomaly of the chaser spacecraft

$$\dot{\theta}_C = \frac{n_C(1 + e_C\cos\theta_C)^2}{(1 - e_C^2)^{\frac{3}{2}}} \tag{3}$$

$$\ddot{\theta}_C = \frac{-2n_C^2 e_C(1 + e_C\cos\theta_C)^3 \sin\theta_C}{(1 - e_C^2)^3} \tag{4}$$

where $n_C = \sqrt{u/a_C^3}$ is the mean orbital angular velocity, a_C the semi-major axe, and e_C the eccentricity of the chaser spacecraft.

However Eq. (1) just only refers to the relationship of the c. m. of the two spacecraft, which will lead to considerable errors about relative translation when the point is not located in the c. m. of the spacecraft.[16] Suppose that P_C is a location of the vision sensor in the chaser spacecraft. Then $\boldsymbol{P}_C$ is a vector directed from P_C to the origin of the reference frame F_C. P_i is an arbitrary feature point in the target spacecraft and $\boldsymbol{P}_i$ is its corresponding vector directed from the origin of the coordinate system F_T to the point P_i. According to vector addition, it is obvious that the following relationship holds:

$$\boldsymbol{P}_i = \boldsymbol{\rho}_i - \boldsymbol{P}_C - \boldsymbol{\rho}_0 \tag{5}$$

where $\boldsymbol{\rho}_0$ is a vector from the chaser's c. m. to the target's c. m.; $\boldsymbol{\rho}_i$ denotes the relative position vector between the vision sensor's location and the feature point with the direction from P_C to P_i. It is straightforward to deduce the first and second time derivatives of $\boldsymbol{P}_i$ and $\boldsymbol{\rho}_i$ in F_C,

$$\dot{\boldsymbol{P}}_i = -\boldsymbol{w} \times \boldsymbol{P}_i \tag{6}$$

$$\ddot{\boldsymbol{P}}_i = \boldsymbol{w} \times (\boldsymbol{w} \times \boldsymbol{P}_i) - \dot{\boldsymbol{w}} \times \boldsymbol{P}_i \tag{7}$$

Eqs. (6) and (7) imply that rotation-translation coupling is able to affect the relative translation. In Ref.[16], it is treated as a kinematic perturbation. This perturbation effect always exists and it is an inherent part of the spacecraft relative motion nothing to do with external disturbation. Specifically, it is more dominant than orbital perturbations at the final phase of RVD. Furthermore, because the target is non-cooperative and the equations of relative translational dynamics need to project onto the reference frame F_C, the time derivatives of relative position vector are different from those given in Ref.[16].

2.2. Relative rotational dynamics

Although quaternion is the most popular approach to represent rigid-body attitude, its four components increase the inconsistent probability of the system to be considered. The Modified Rodrigues parameter is just composed of three parts and it is the minimum parameters to describe the attitude of rigid-body. Suppose $\boldsymbol{\sigma} = [\sigma_1, \sigma_2, \sigma_3]^T$ to be a Modified Rodrigues parameter[21] which denotes the reference frame F_C relative to F_T and then the attitude matrix is given by

$$\boldsymbol{R}_{CT}(\boldsymbol{\sigma}) = \boldsymbol{I} - \frac{4(1 - \boldsymbol{\sigma}^T\boldsymbol{\sigma})}{(1 + \boldsymbol{\sigma}^T\boldsymbol{\sigma})^2}[\boldsymbol{\sigma}\times] + \frac{8}{(1 + \boldsymbol{\sigma}^T\boldsymbol{\sigma})^2}[\boldsymbol{\sigma}\times]^2 \tag{8}$$

where $\boldsymbol{R}_{CT}(\boldsymbol{\sigma})$ is able to transform a vector from frame F_T to frame F_C. The kinematic equation by the Modified Rodrigues parameters can be shown by

$$\dot{\boldsymbol{\sigma}} = \frac{1}{4}[(1 - \boldsymbol{\sigma}^T\boldsymbol{\sigma})\boldsymbol{I} + 2[\boldsymbol{\sigma}\times] + 2\boldsymbol{\sigma}\boldsymbol{\sigma}^T]\boldsymbol{w} \tag{9}$$

where $\boldsymbol{w}$ expresses the angular velocity of frame F_C to frame F_T, consequently

$$\boldsymbol{w} = \boldsymbol{w}_{IC} - \boldsymbol{w}_{IT} \tag{10}$$

where $\boldsymbol{w}_{IC}$ and $\boldsymbol{w}_{IT}$ are the angular velocities of the chaser and target spacecraft relative to the frame F_I, respectively. The first time derivative of Eq. (10) in the frame F_I leads to

$$\left.\frac{d\boldsymbol{w}}{dt}\right|_I = \left.\frac{d\boldsymbol{w}_{IC}}{dt}\right|_I - \left.\frac{d\boldsymbol{w}_{IT}}{dt}\right|_I \tag{11}$$

And according to Coriolis' theorem, it can be directly obtained that

$$\left.\frac{d\boldsymbol{w}}{dt}\right|_I = \left.\frac{d\boldsymbol{w}}{dt}\right|_C + \boldsymbol{w}_{IC} \times \boldsymbol{w} \tag{12}$$

In combination with Eqs. (11) and (12), it easily gets

$$\left.\frac{\mathrm{d}\boldsymbol{w}}{\mathrm{d}t}\right|_{\mathrm{C}}=\left.\frac{\mathrm{d}\boldsymbol{w}_{\mathrm{IC}}}{\mathrm{d}t}\right|_{\mathrm{I}}-\left.\frac{\mathrm{d}\boldsymbol{w}_{\mathrm{IT}}}{\mathrm{d}t}\right|_{\mathrm{I}}-\boldsymbol{w}_{\mathrm{IC}}\times\boldsymbol{w} \tag{13}$$

Since $\left.\frac{\mathrm{d}\boldsymbol{w}_{\mathrm{IC}}}{\mathrm{d}t}\right|_{\mathrm{I}}=\left.\frac{\mathrm{d}\boldsymbol{w}_{\mathrm{IC}}}{\mathrm{d}t}\right|_{\mathrm{C}}$ and $\left.\frac{\mathrm{d}\boldsymbol{w}_{\mathrm{IT}}}{\mathrm{d}t}\right|_{\mathrm{I}}=\left.\frac{\mathrm{d}\boldsymbol{w}_{\mathrm{IT}}}{\mathrm{d}t}\right|_{\mathrm{T}}$, Eq. (13) can be written as

$$\left(\left.\frac{\mathrm{d}\boldsymbol{w}}{\mathrm{d}t}\right|_{\mathrm{C}}\right)^{\mathrm{C}}=\left(\left.\frac{\mathrm{d}\boldsymbol{w}_{\mathrm{IC}}}{\mathrm{d}t}\right|_{\mathrm{C}}\right)^{\mathrm{C}}-\boldsymbol{R}_{\mathrm{CT}}\left(\left.\frac{\mathrm{d}\boldsymbol{w}_{\mathrm{IT}}}{\mathrm{d}t}\right|_{\mathrm{T}}\right)^{\mathrm{T}}-\boldsymbol{w}_{\mathrm{IC}}^{\mathrm{C}}\times\boldsymbol{w}^{\mathrm{C}} \tag{14}$$

Assume that $\boldsymbol{H}$ and $\boldsymbol{N}$ are the total momentum and external torque of a rigid-body, respectively, then for the chaser spacecraft,

$$\frac{\mathrm{d}\boldsymbol{H}_{\mathrm{C}}}{\mathrm{d}t}=\boldsymbol{I}_{\mathrm{C}}\left.\frac{\mathrm{d}\boldsymbol{w}_{\mathrm{IC}}}{\mathrm{d}t}\right|_{\mathrm{C}}+\boldsymbol{w}_{\mathrm{IC}}\times\boldsymbol{I}_{\mathrm{C}}\boldsymbol{w}_{\mathrm{IC}}=\boldsymbol{N}_{\mathrm{C}} \tag{15}$$

and for the target spacecraft,

$$\frac{\mathrm{d}\boldsymbol{H}_{\mathrm{T}}}{\mathrm{d}t}=\boldsymbol{I}_{\mathrm{T}}\left.\frac{\mathrm{d}\boldsymbol{w}_{\mathrm{IT}}}{\mathrm{d}t}\right|_{\mathrm{T}}+\boldsymbol{w}_{\mathrm{IT}}\times\boldsymbol{I}_{\mathrm{T}}\boldsymbol{w}_{\mathrm{IT}}=\boldsymbol{N}_{\mathrm{T}} \tag{16}$$

where $\boldsymbol{I}_{\mathrm{C}}$ and $\boldsymbol{I}_{\mathrm{T}}$ are the inertia tensor of the chaser and target spacecraft, respectively. Notably, since the target is non-cooperative, $\boldsymbol{I}_{\mathrm{T}}$ is unknown. And this is a major consideration to settle in this paper. Furthermore, it is considered that the target is just disturbed by environmental torque (e. g., the gravity gradient torque) without control moment. Consequently, $\boldsymbol{N}_{\mathrm{T}}$ is able to be considered as a zero-mean white Gaussian process noise with covariance $\boldsymbol{Q}_{\mathrm{T}}$. Since $\boldsymbol{H}=\boldsymbol{I}\boldsymbol{w}$ and combining with Eqs. (14)–(16), the relative rotational dynamic is described by

$$\begin{aligned}\left(\left.\frac{\mathrm{d}\boldsymbol{w}}{\mathrm{d}t}\right|_{\mathrm{C}}\right)^{\mathrm{C}}&=\boldsymbol{I}_{\mathrm{C}}^{-1}\left(\boldsymbol{N}_{\mathrm{C}}-\boldsymbol{w}_{\mathrm{IC}}^{\mathrm{C}}\times\boldsymbol{I}_{\mathrm{C}}\boldsymbol{w}_{\mathrm{IC}}^{\mathrm{C}}\right)\\&\quad-\boldsymbol{R}_{\mathrm{CT}}\boldsymbol{I}_{\mathrm{T}}^{-1}\left(\boldsymbol{N}_{\mathrm{T}}-\boldsymbol{w}_{\mathrm{IT}}^{\mathrm{T}}\times\boldsymbol{I}_{\mathrm{T}}\boldsymbol{w}_{\mathrm{IT}}^{\mathrm{T}}\right)-\boldsymbol{w}_{\mathrm{IC}}^{\mathrm{C}}\times\boldsymbol{w}^{\mathrm{C}}\end{aligned} \tag{17}$$

Furthermore, $\boldsymbol{w}_{\mathrm{IT}}$ is unknown for a non-cooperative target and then Eq. (17) can be written as

$$\begin{aligned}\left(\left.\frac{\mathrm{d}\boldsymbol{w}}{\mathrm{d}t}\right|_{\mathrm{C}}\right)^{\mathrm{C}}&=\boldsymbol{I}_{\mathrm{C}}^{-1}\left(\boldsymbol{N}_{\mathrm{C}}-\boldsymbol{w}_{\mathrm{IC}}^{\mathrm{C}}\times\boldsymbol{I}_{\mathrm{C}}\boldsymbol{w}_{\mathrm{IC}}^{\mathrm{C}}\right)\\&\quad-\boldsymbol{R}_{\mathrm{CT}}\boldsymbol{I}_{\mathrm{T}}^{-1}\left(\boldsymbol{N}_{\mathrm{T}}-\boldsymbol{R}_{\mathrm{CT}}^{\mathrm{T}}\left(\boldsymbol{w}_{\mathrm{IC}}^{\mathrm{C}}-\boldsymbol{w}^{\mathrm{C}}\right)\times\boldsymbol{I}_{\mathrm{T}}\boldsymbol{R}_{\mathrm{CT}}^{\mathrm{T}}\left(\boldsymbol{w}_{\mathrm{IC}}^{\mathrm{C}}-\boldsymbol{w}^{\mathrm{C}}\right)\right)\\&\quad-\boldsymbol{w}_{\mathrm{IC}}^{\mathrm{C}}\times\boldsymbol{w}^{\mathrm{C}}\end{aligned} \tag{18}$$

3. Rendezvous and docking for non-cooperative target

3.1. Problem statement

In this paper, we aim to estimate the relative states of non-cooperative target at the final phase of RVD. A set of points which are acquired by stereo vision are the main external data source, then the state vector $\boldsymbol{x}$ is

$$\boldsymbol{x}=\left[\boldsymbol{\rho}_0^{\mathrm{T}},\dot{\boldsymbol{\rho}}_0^{\mathrm{T}},\boldsymbol{\sigma}^{\mathrm{T}},\boldsymbol{w}^{\mathrm{T}},\boldsymbol{P}_1^{\mathrm{T}},\boldsymbol{P}_2^{\mathrm{T}},\ldots,\boldsymbol{P}_N^{\mathrm{T}},\dot{\boldsymbol{P}}_1^{\mathrm{T}},\dot{\boldsymbol{P}}_2^{\mathrm{T}},\ldots,\dot{\boldsymbol{P}}_N^{\mathrm{T}}\right]^{\mathrm{T}}\in\mathbf{R}^{12+6N} \tag{19}$$

where $\boldsymbol{P}_i$ is the vector of feature point in Eq. (5) and its corresponding image coordinates are assumed to be processed by speeded-up robust features (SURF) descriptor which is distinctive and robust.[22] Then, consider a nonlinear continuous-time dynamical system with additive noise described by

$$\dot{\boldsymbol{x}}=\boldsymbol{f}(\boldsymbol{x})+\boldsymbol{v} \tag{20}$$

where $\boldsymbol{v}$ is zero-mean white Gaussian process noise with covariance $\boldsymbol{Q}$; $\boldsymbol{f}(\boldsymbol{x})$ is a nonlinear vector-valued function and its explicit form is referred to Eqs. (1), (6), (7), (9) and (18). Due to the fact that the nonlinear dynamical system is continuous, Eq. (20) is not suitable for computer to calculate its numerical solutions. Fortunately, a method is given by Crassidis to discretize the continuous-time system and a more detail description of the method can be found in Ref.[23].

3.2. Observation model

Suppose that a stereo vision system is assembled at the chaser spacecraft (see Fig. 2). It consists of a pair of completely parallel cameras with focal length f. And the left one which is located at the point P_{C} is the center of the system, keeping a baseline distance B away from the right one. Moreover, it is assumed that the reference of the vision system consists with the body-fixed frame of the chaser spacecraft. Then, an arbitrary feature point $\boldsymbol{P}_i$ on the target spacecraft satisfies

$$\boldsymbol{\rho}_i=\boldsymbol{R}_{\mathrm{CT}}\boldsymbol{P}_i+\boldsymbol{\rho}_0+\boldsymbol{P}_{\mathrm{C}} \tag{21}$$

where $\boldsymbol{\rho}_i=[\rho_{ix},\rho_{iy},\rho_{iz}]^{\mathrm{T}}$ is a vector of line sight between the left camera and the feature point $\boldsymbol{P}_i$. Project the vector $\boldsymbol{\rho}_i$ onto the image plane and the relationship between $\mathbf{R}^3$ and $\mathbf{R}^2$ is described by

$$\begin{cases}x_{i\mathrm{L}}=f\dfrac{\rho_{ix}}{\rho_{iz}}\\[2mm] x_{i\mathrm{R}}=f\dfrac{(\rho_{ix}-B)}{\rho_{iz}}\\[2mm] y_{i\mathrm{L}}=y_{i\mathrm{R}}=f\dfrac{\rho_{iy}}{\rho_{iz}}\end{cases} \tag{22}$$

where $x_{i\mathrm{L}}$ and $y_{i\mathrm{L}}$ constitute a coordinate of the point $\boldsymbol{P}_i$ on image plane of the left camera; $x_{i\mathrm{R}}$ and $y_{i\mathrm{R}}$ constitute a coordinate of the point $\boldsymbol{P}_i$ on image plane of the right camera. Consequently, the observation model can be written as

$$\boldsymbol{z}_{ik}=\boldsymbol{h}_i(x_k)+\boldsymbol{n}_{ik}\qquad i=1,2,\cdots,N \tag{23}$$

where $\boldsymbol{n}_{ik}$ is a zero-mean white Gaussian measurement noise with covariance $\boldsymbol{R}$; $\boldsymbol{z}_{ik}$ is an observation vector which is captured by vision sensors; $\boldsymbol{h}_i(x_k)$ is defined as $\boldsymbol{h}_i(x_k)=[x_{i\mathrm{R}},y_{i\mathrm{R}},x_{i\mathrm{L}},y_{i\mathrm{L}}]^{\mathrm{T}}$.

Eqs. (20) and (23) jointly constitute the system model to be processed in this paper. It is notable that the vector of feature point is regarded as a part of the state vector. Accordingly, there is no need to know the precise position of feature point

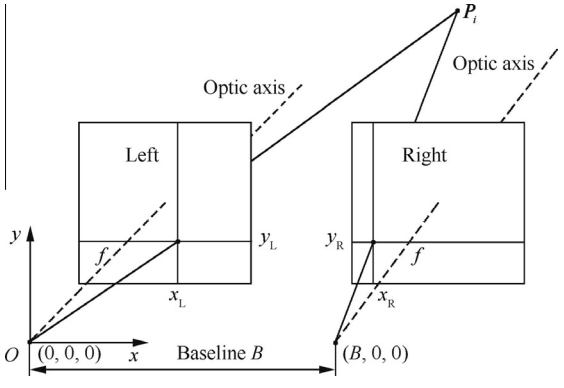

Fig. 2 Stereo vision system.

in the reference frame F_{T}. Furthermore, it is not required to capture all the feature points of the target spacecraft. Namely, it means that the proposed algorithm is suitable for the severe conditions of light (e. g., shadow and occlusion).

4. Estimation methodology

4.1. Dealing with unknown inertia tensor

In this section, the InCKF is introduced to deal with the unknown inertia tensor of target spacecraft. This novel filter we proposed is presented in our previous work[24], and here we employ it to estimate the states of relative navigation at the final phase of RVD. Furthermore, algorithm of the InCKF is extended in comparison with Ref.[24]. The InCKF consists of multiple CKFs and a maximum a posteriori (MAP) calculator. The output of CKFs is taken as the input of MAP calculator to identify which hypothesis about inertia tensor is the best in the present moment. And then, the output of MAP calculator about inertia tensor is treated as a reference input of CKFs. Consequently, the InCKF we proposed is a closed-loop structure. Details of the InCKF are as follows.

The multiple CKFs of the novel approach work concurrently and each is calculated to approximate

$$\hat{\boldsymbol{x}}_k(\boldsymbol{I}_{\mathrm{T}\_j}) \approx E\{\boldsymbol{x}_k|\boldsymbol{\Xi}_{1:k},\boldsymbol{I}_{\mathrm{T}\_j}\} \tag{24}$$

where $\boldsymbol{\Xi}_k = [\boldsymbol{z}_{1k}^{\mathrm{T}}, \boldsymbol{z}_{2k}^{\mathrm{T}}, \ldots, \boldsymbol{z}_{Nk}^{\mathrm{T}}]^{\mathrm{T}}$ is the observation vector at time k and $\hat{\boldsymbol{x}}_k(\boldsymbol{I}_{\mathrm{T}\_j})$ the estimation of CKF with a hypothetical inertial tensor $\boldsymbol{I}_{\mathrm{T}\_j}$. The details of inertia estimation are derived in the following text. It takes Bayes' rule to estimate the inertial tensor $\boldsymbol{I}_{\mathrm{T}\_j}$ in this paper. And its posterior probability can be written as

$$p(\boldsymbol{I}_{\mathrm{T}\_j}|\boldsymbol{\Xi}_{1:k}) \propto p(\boldsymbol{\Xi}_{1:k}|\boldsymbol{I}_{\mathrm{T}\_j})p(\boldsymbol{I}_{\mathrm{T}} = \boldsymbol{I}_{\mathrm{T}\_j}) \tag{25}$$

where $p(\boldsymbol{\Xi}_{1:k}|\boldsymbol{I}_{\mathrm{T}\_j})$ is the likelihood of measurements for a period of time conditioned on the inertial tensor $\boldsymbol{I}_{\mathrm{T}\_j}$; $p(\boldsymbol{I}_{\mathrm{T}} = \boldsymbol{I}_{\mathrm{T}\_j})$ is the prior probability about inertial tensor. Recalling multiplication rule, it can be directly obtained that

$$p(\boldsymbol{\Xi}_{1:k}|\boldsymbol{I}_{\mathrm{T}\_j}) = p(\boldsymbol{\Xi}_1|\boldsymbol{I}_{\mathrm{T}\_j})\prod_{i=2}^{k} p(\boldsymbol{\Xi}_i|\boldsymbol{I}_{\mathrm{T}\_j}, \boldsymbol{\Xi}_{1:i-1}) \tag{26}$$

And the factor $p(\boldsymbol{\Xi}_i|\boldsymbol{I}_{\mathrm{T}\_j}, \boldsymbol{\Xi}_{1:i-1})$ can be expanded by

$$\begin{aligned} p(\boldsymbol{\Xi}_i|\boldsymbol{I}_{\mathrm{T}\_j}, \boldsymbol{\Xi}_{1:i-1}) &= \iint p(\boldsymbol{\Xi}_i|\boldsymbol{x}_i)p(\boldsymbol{x}_i|\boldsymbol{x}_{i-1}, \boldsymbol{I}_{\mathrm{T}\_j})p(\boldsymbol{x}_{i-1}|\boldsymbol{\Xi}_{1:i-1})\mathrm{d}\boldsymbol{x}_i\mathrm{d}\boldsymbol{x}_{i-1} \\ &= \int p(\boldsymbol{\Xi}_i|\boldsymbol{x}_i)p(\boldsymbol{x}_i|\boldsymbol{\Xi}_{1:i-1}, \boldsymbol{I}_{\mathrm{T}\_j})\mathrm{d}\boldsymbol{x}_i \\ &= E\{p(\boldsymbol{\Xi}_i|\boldsymbol{x}_i)|\boldsymbol{\Xi}_{1:i-1}, \boldsymbol{I}_{\mathrm{T}\_j}\} \end{aligned} \tag{27}$$

where $p(\boldsymbol{x}_i|\boldsymbol{x}_{i-1}, \boldsymbol{I}_{\mathrm{T}\_j})$ is the density function of transition probability and it is evaluated by states Eq. (20).

In Ref.[24], we proposed two methods to approximate the likelihood probability which are based on second-order Stirling's interpolation (SI2)[25] and unscented transformation (UT)[26], respectively. In this section, another method based on spherical-radial rule is proposed to estimate the likelihood probability of inertial tensor.

4.2. Approximation based on third-degree spherical-radial rule

Third-degree spherical-radial (SR) rule[20]: consider a multi-dimensional integral of Gaussian weight $\boldsymbol{I}_{\mathcal{N}}(\boldsymbol{f}) = \int_{\mathbf{R}^n} \boldsymbol{f}(\boldsymbol{x})\mathcal{N}(\boldsymbol{x}; \hat{\boldsymbol{x}}, \boldsymbol{P})\mathrm{d}\boldsymbol{x}$, and then the approximation of $\boldsymbol{I}_{\mathcal{N}}(\boldsymbol{f})$ by the third-degree spherical-radial rule is

$$\begin{aligned} \int_{\mathbf{R}^n} \boldsymbol{f}(\boldsymbol{x})\mathcal{N}(\boldsymbol{x}; \hat{\boldsymbol{x}}, \boldsymbol{P})\mathrm{d}\boldsymbol{x} &= \int_{\mathbf{R}^n} \boldsymbol{f}(\boldsymbol{S}\boldsymbol{\xi}_d + \hat{\boldsymbol{x}})\mathcal{N}(\boldsymbol{x}; \boldsymbol{0}, \boldsymbol{I})\mathrm{d}\boldsymbol{x} \\ &\approx \sum_{d=1}^{2n} w\boldsymbol{f}(\boldsymbol{S}\boldsymbol{\xi}_d + \hat{\boldsymbol{x}}) \end{aligned} \tag{28}$$

where $\boldsymbol{S}$ is the square-root of covariance matrix $\boldsymbol{P}$; $w = \dfrac{1}{2n}$ denotes weighted factor; $\boldsymbol{\xi}_d$ is dth column of the cubature-point set $\{\boldsymbol{\xi}_d\}$. And the form of $\{\boldsymbol{\xi}_d\}$ is

$$\{\boldsymbol{\xi}_d\} = \sqrt{n}\left\{\begin{bmatrix}1\\0\\\vdots\\0\end{bmatrix}, \begin{bmatrix}0\\1\\\vdots\\0\end{bmatrix}, \cdots, \begin{bmatrix}0\\0\\\vdots\\1\end{bmatrix}, \begin{bmatrix}-1\\0\\\vdots\\0\end{bmatrix}, \begin{bmatrix}0\\-1\\\vdots\\0\end{bmatrix}, \cdots, \begin{bmatrix}0\\0\\\vdots\\-1\end{bmatrix}\right\} \tag{29}$$

Using third-degree spherical-radial rule, the factor $p(\boldsymbol{\Xi}_i|\boldsymbol{I}_{\mathrm{T}\_j}, \boldsymbol{\Xi}_{1:i-1})$ of right hand side in Eq. (26) can be approximated by

$$\begin{aligned} p(\boldsymbol{\Xi}_i|\boldsymbol{\Xi}_{1:i-1}, \boldsymbol{I}_{\mathrm{T}\_j}) &= \iint p(\boldsymbol{\Xi}_i|\boldsymbol{x}_i)p(\boldsymbol{x}_i|\boldsymbol{x}_{i-1}, \boldsymbol{I}_{\mathrm{T}\_j})p(\boldsymbol{x}_{i-1}|\boldsymbol{\Xi}_{1:i-1})\mathrm{d}\boldsymbol{x}_i\mathrm{d}\boldsymbol{x}_{i-1} \\ &= \int p(\boldsymbol{\Xi}_i|\boldsymbol{x}_i)p(\boldsymbol{x}_i|\boldsymbol{I}_{\mathrm{T}\_j}, \boldsymbol{\Xi}_{1:i-1})\mathrm{d}\boldsymbol{x}_i \\ &= \int p(\boldsymbol{\Xi}_i|\boldsymbol{x}_i)\mathcal{N}(\boldsymbol{x}_i; \hat{\boldsymbol{x}}_i^-(\boldsymbol{I}_{\mathrm{T}\_j}), \boldsymbol{P}_i^-)\mathrm{d}\boldsymbol{x}_i \\ &= \int p(\boldsymbol{\Xi}_i|\boldsymbol{S}_i^-\boldsymbol{\xi}_d + \hat{\boldsymbol{x}}_i^-(\boldsymbol{I}_{\mathrm{T}\_j}))\mathcal{N}(\boldsymbol{x}_i; \boldsymbol{0}, \boldsymbol{I})\mathrm{d}\boldsymbol{x}_i \\ &\approx \sum_{d=1}^{2n} wp\left(\boldsymbol{\Xi}_i|\boldsymbol{S}_i^-\boldsymbol{\xi}_d + \hat{\boldsymbol{x}}_i^-(\boldsymbol{I}_{\mathrm{T}\_j})\right) \end{aligned} \tag{30}$$

where $\boldsymbol{S}_i^-$ is the square-root of the predicated covariance $\boldsymbol{P}_i^-$ at time i. And then, Eq. (26) can be approximated by

$$\begin{aligned} p(\boldsymbol{\Xi}_{1:k}|\boldsymbol{I}_{\mathrm{T}\_j}) &\approx \prod_{i=1}^{k}\left(\sum_{d=1}^{2n} wp(\boldsymbol{\Xi}_i|\boldsymbol{S}_i^-\boldsymbol{\xi}_d + \hat{\boldsymbol{x}}_i^-(\boldsymbol{I}_{\mathrm{T}\_j}))\right) \\ &= \prod_{i=1}^{k}\left(\sum_{d=1}^{2n} w\left(\prod_{m=1}^{N} p(\boldsymbol{z}_{mi} - \boldsymbol{h}_m(\boldsymbol{S}_i^-\boldsymbol{\xi}_d + \hat{\boldsymbol{x}}_i^-(\boldsymbol{I}_{\mathrm{T}\_j})))\right)\right) \\ &= \prod_{i=1}^{k}\left(\sum_{d=1}^{2n} w\left(\prod_{m=1}^{N} \frac{1}{\sqrt{|2\pi\boldsymbol{R}|}}\exp\left(-\frac{(\boldsymbol{z}_{mi} - \boldsymbol{h}_m(\boldsymbol{S}_i^-\boldsymbol{\xi}_d + \hat{\boldsymbol{x}}_i^-(\boldsymbol{I}_{\mathrm{T}\_j})))^{\mathrm{T}}\boldsymbol{R}^{-1}(\boldsymbol{z}_{mi} - \boldsymbol{h}_m(\boldsymbol{S}_i^-\boldsymbol{\xi}_d + \hat{\boldsymbol{x}}_i^-(\boldsymbol{I}_{\mathrm{T}\_j})))}{2}\right)\right)\right) \\ &= \prod_{i=1}^{k}\frac{1}{\sqrt{|2\pi\boldsymbol{R}|^N}}\left(\sum_{d=1}^{2n} w\left(\exp\left(\frac{-\sum_{m=1}^{N}(\boldsymbol{z}_{mi} - \boldsymbol{h}_m(\boldsymbol{S}_i^-\boldsymbol{\xi}_d + \hat{\boldsymbol{x}}_i^-(\boldsymbol{I}_{\mathrm{T}\_j})))^{\mathrm{T}}\boldsymbol{R}^{-1}(\boldsymbol{z}_{mi} - \boldsymbol{h}_m(\boldsymbol{S}_i^-\boldsymbol{\xi}_d + \hat{\boldsymbol{x}}_i^-(\boldsymbol{I}_{\mathrm{T}\_j})))}{2}\right)\right)\right) \end{aligned} \tag{31}$$

Let $M_{\mathrm{SR}} := \dfrac{-\sum_{m=1}^{N}(\boldsymbol{z}_{mi} - \boldsymbol{h}_m(\boldsymbol{S}_i^-\boldsymbol{\xi}_d + \hat{\boldsymbol{x}}_i^-(\boldsymbol{I}_{\mathrm{T}\_j})))^{\mathrm{T}}\boldsymbol{R}^{-1}(\boldsymbol{z}_{mi} - \boldsymbol{h}_m(\boldsymbol{S}_i^-\boldsymbol{\xi}_d + \hat{\boldsymbol{x}}_i^-(\boldsymbol{I}_{\mathrm{T}\_j})))}{2}$; $\exp(\bullet)$ is also approximated by the second order Taylor expansion, then

$$p(\boldsymbol{\Xi}_{1:k}|\boldsymbol{I}_{\mathrm{T}\_j}) \approx \prod_{i=1}^{k}\frac{1}{\sqrt{|2\pi\boldsymbol{R}|^N}}\left(\sum_{d=1}^{2n} w\left(1 + M_{\mathrm{SR}} + \frac{M_{\mathrm{SR}}^2}{2}\right)\right) \tag{32}$$

Let

$$\hat{p}_{\mathrm{SR}}(\boldsymbol{\Xi}_{1:k}|\boldsymbol{I}_{\mathrm{T}\_j}) := \prod_{i=1}^{k}\frac{1}{\sqrt{|2\pi\boldsymbol{R}|^N}}\left(\sum_{d=1}^{2n} w\left(1 + M_{\mathrm{SR}} + \frac{M_{\mathrm{SR}}^2}{2}\right)\right) \tag{33}$$

Take logarithm of Eq. (33), which yields

$$\begin{aligned}\ln \hat{p}_{\mathrm{SR}}(\boldsymbol{\Xi}_{1:k}|\boldsymbol{I}_{\mathrm{T}\_j}) &= \ln\left(\prod_{i=1}^{k}\frac{1}{\sqrt{|2\pi\boldsymbol{R}|^{N}}}\left(\sum_{d=1}^{2n}w\left(1+M_{\mathrm{SR}}+\frac{M_{\mathrm{SR}}^{2}}{2}\right)\right)\right)\\ &= \sum_{i=1}^{k}\ln\frac{1}{\sqrt{|2\pi\boldsymbol{R}|^{N}}}\left(\sum_{d=1}^{2n}w\left(1+M_{\mathrm{SR}}+\frac{M_{\mathrm{SR}}^{2}}{2}\right)\right)\end{aligned} \tag{34}$$

And finally, we take MAP to estimate the most probable inertial tensor

$$\hat{\boldsymbol{I}}_{\mathrm{MAP}} = \arg\max_{\boldsymbol{I}_{\mathrm{T}\_j}\in\boldsymbol{I}_{\mathrm{T}}} \ln \hat{p}_{(\bullet)}(\boldsymbol{\Xi}_{1:k}|\boldsymbol{I}_{\mathrm{T}\_j}) + \ln p(\boldsymbol{I}_{\mathrm{T}} = \boldsymbol{I}_{\mathrm{T}\_j}) \tag{35}$$

where $\ln \hat{p}_{(\bullet)}(\boldsymbol{\Xi}_{1:k}|\boldsymbol{I}_{\mathrm{T}\_k})$ denotes Eq. (34). In addition, if the precision of the prior probability $P(\boldsymbol{I}_{\mathrm{T}})$ is rough, it can be modified by posterior estimation, that is

$$\hat{\boldsymbol{I}}_{\mathrm{MAP}} = \arg\max_{\boldsymbol{I}_{\mathrm{T}\_j}\in\boldsymbol{I}_{\mathrm{T}}} \ln \hat{p}_{(\bullet)}(\boldsymbol{\Xi}_{1:k}|\boldsymbol{I}_{\mathrm{T}\_j}) + \ln \hat{p}_{(\bullet)}(\boldsymbol{I}_{\mathrm{MAP}}|\boldsymbol{\Xi}_{1:k}) \tag{36}$$

where

$$\hat{p}_{(\bullet)}(\boldsymbol{I}_{\mathrm{MAP}}|\boldsymbol{\Xi}_{1:k}) = \hat{p}_{(\bullet)}(\boldsymbol{\Xi}_{1:k}|\boldsymbol{I}_{\mathrm{MAP}})p(\boldsymbol{I}_{\mathrm{T}} = \boldsymbol{I}_{\mathrm{MAP}}) \tag{37}$$

and $\hat{p}_{(\bullet)}(\boldsymbol{\Xi}_{1:k}|\boldsymbol{I}_{\mathrm{MAP}})$ denotes Eq. (33). Based on the above discussions, the algorithm of InCKF based on spherical-radial rule is summarized as follows.

Algorithm 1: Main Framework of InCKF Algorithm

1: Initialization: $\hat{\boldsymbol{x}}_0 = \boldsymbol{0}$, $\hat{\boldsymbol{I}}_{\mathrm{MAP}} = \boldsymbol{I}$, $k = 0$;
2: **While** time $k <$ finish time **do**
3: Sample $\boldsymbol{I}_{\mathrm{T}\_j}$ from $p(\boldsymbol{I}_{\mathrm{T}})$, $j = 1, 2, \ldots N_{\mathrm{I}}$;
4: Let $\boldsymbol{I}_{\mathrm{T}\_0} := \hat{\boldsymbol{I}}_{\mathrm{MAP}}$;
6: **for** $j = 0, 1, \ldots N_{\mathrm{I}}$ do
7: Implement CKF using an assumptive inertial tensor $\boldsymbol{I}_{\mathrm{T}\_j}$ to acquire $[\hat{\boldsymbol{x}}_k^{-}(\boldsymbol{I}_{\mathrm{T}\_j})$ and $\hat{\boldsymbol{x}}_k(\boldsymbol{I}_{\mathrm{T}\_j})$;
8: Compute $\ln \hat{p}(\boldsymbol{\Xi}_{1:k}|\boldsymbol{I}_{\mathrm{T}_k})$using Eq. (34);
9: **end for**
10: Compute the most probable inertial tensor $\hat{\boldsymbol{I}}_{\mathrm{MAP}}$ using Eq. (36);
11: Set the prior probability $p(\boldsymbol{I}_{\mathrm{T}}) = \hat{p}_{(\bullet)}(\boldsymbol{I}_{\mathrm{MAP}}|\boldsymbol{\Xi}_{1:k})$ by Eq. (37);
12: Set the algorithm's output as $\hat{\boldsymbol{x}}_k(\hat{\boldsymbol{I}}_{\mathrm{MAP}})$;
13: $k = k + 1$;
14: **end while**

5. Simulation

In this section, two numerical examples are conducted for evaluating the performance of the proposed estimator. Both of the two examples refer to the situation about the final phase of RVD. The first example compares the system model which considers translation-rotation coupling with the uncouple model. In this example, the inertial tensor of target spacecraft is known and the relative states are estimated by CKF. The second example is the major consideration, in which the inertial tensor of target spacecraft is unknown. And the motivation behind this example is to elucidate that the proposed estimator is more robust than EKF to deal with the relative estimation about unknown inertial tensor. The parameters of chaser spacecraft are shown in Table 1. The vision parameters used here are obtained from the Falcon 4M30 camera.

In the following examples, we suppose that the locations of the feature points on the target spacecraft are subject to uniform distribution,

$$\boldsymbol{P}_i \sim \boldsymbol{U}(-1.5\ \mathrm{m}, 1.5\ \mathrm{m}) \tag{38}$$

5.1. Example I

In the first simulation example, the inertial tensor of target spacecraft is known and its value is the same with that of chaser spacecraft. The initial states are set as follows:

$$\boldsymbol{\rho}_0(0) = [25, 25, 50]^{\mathrm{T}} \quad \mathrm{m} \tag{39}$$

$$\dot{\boldsymbol{\rho}}_0(0) = [-0.3889, -0.4392, -0.8264]^{\mathrm{T}} \quad \mathrm{m/s} \tag{40}$$

$$\boldsymbol{\sigma}(0) = [0, 0, 0] \tag{41}$$

$$\boldsymbol{w}(0) = [0.1n(0), 0.1n(0), 2n(0)] \tag{42}$$

where $\boldsymbol{\rho}_0(0)$ is the initial relative position between chaser and target spacecraft, $\dot{\boldsymbol{\rho}}_0(0)$ the initial relative velocity, $\boldsymbol{\sigma}(0)$ the initial relative attitude, $\boldsymbol{w}(0)$ the initial relative angular velocity and $n(0)$ can be obtained from Eq. (3). In addition, the initial states about the feature points in the couple model are given by

$$\dot{\boldsymbol{P}}_i(0) = -\boldsymbol{w}(0) \times \boldsymbol{P}_i \tag{43}$$

$$\ddot{\boldsymbol{P}}_i(0) = \boldsymbol{w}(0) \times (\boldsymbol{w}(0) \times \boldsymbol{P}_i) - \dot{\boldsymbol{w}}(0) \times \boldsymbol{P}_i \tag{44}$$

And the estimation error eFP of the feature point locations is defined as

$$\begin{cases}\mathrm{eFP}_i = \sqrt{(P_{ix} - \hat{P}_{ix})^2 + (P_{iy} - \hat{P}_{iy})^2 + (P_{iz} - \hat{P}_{iz})^2} & i = 1, 2, \ldots, N\\ \mathrm{eFP} = \sum_{i=1}^{N}\mathrm{eFP}_i\end{cases} \tag{45}$$

The comparisons of states' estimation between couple model and uncouple model are shown in Figs. 3–7. Firstly in Figs. 3–6, though the state estimation of uncouple model at the initial phase is more fluctuant than that of couple model, their final results are close. It implies that couple model is able to estimate the relative states with the same accuracy as uncouple model. And it means that CKF can elegantly handle highly nonlinear systems and it is still consistent with respect to a higher dimensional system. Secondly, the biggest advantage of couple model is shown in Fig. 7. It is obvious that couple model could reach much more accuracy than uncouple model

Table 1 Parameters of chaser spacecraft.

Parameter	Value
Eccentric orbit parameter	$a_{\mathrm{C}} = 9000$ km, $e_{\mathrm{C}} = 0.2$, $\Omega_{\mathrm{C}} = 45°$, $i_{\mathrm{C}} = 30°$, $\omega_{\mathrm{C}} = 30°$, $\theta_{\mathrm{C}}(0) = 0°$
Inertia moment	$\boldsymbol{I}_{\mathrm{C}} = \begin{bmatrix}500 & 0 & 0\\ 0 & 550 & 0\\ 0 & 0 & 600\end{bmatrix}$ kg · m^2
Vision system	$f = 12$ mm, $B = 1$ m, $\boldsymbol{P}_{\mathrm{C}} = [1.5, 1.5, 0]^{\mathrm{T}}$ m, resolution : 2352 × 1728 pixels, 7.4 μm × 7.4 μm size

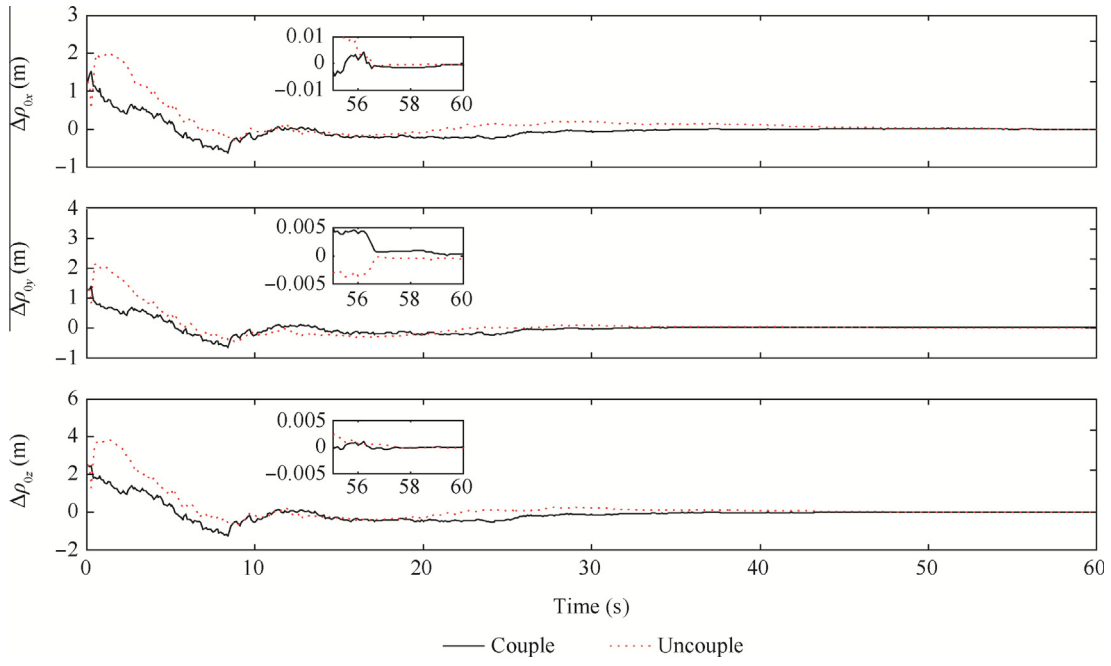

Fig. 3 Position estimation errors.

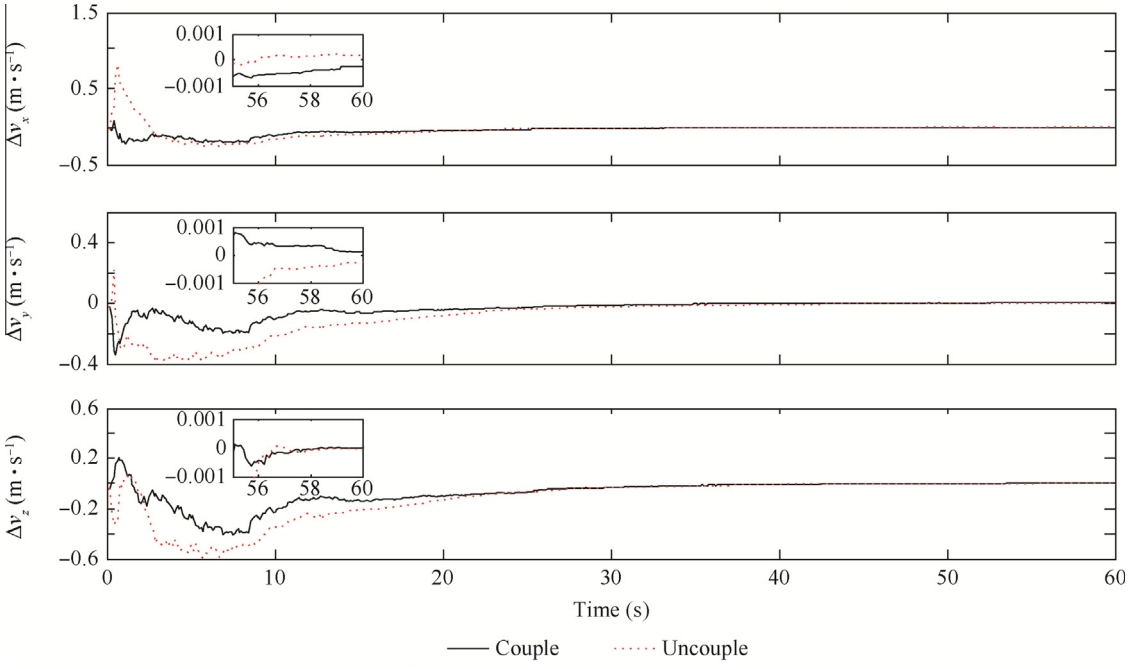

Fig. 4 Velocity estimation errors.

about position of feature points. The result of uncouple model is consistent with its initial error for the reason that its states do not refer to the dynamics of the feature points. And the structure recovery of target spacecraft is affected by the estimation precision of the feature points. From the above analysis, we can see that the couple model is more suitable than uncouple model to estimate relative sates at the final phase of RVD with respect to non-cooperative target.

5.2. Example II

In this example, InCKF is compared with EKF about relative estimation of unknown inertial tensor. It is supposed that the posteriori probability about inertial tensor of target spacecraft is subject to uniform distribution

$$\boldsymbol{I}_{\mathrm{T}} \sim \boldsymbol{U}(450\ \mathrm{kg}\cdot\mathrm{m}^2,\ 600\ \mathrm{kg}\cdot\mathrm{m}^2) \tag{46}$$

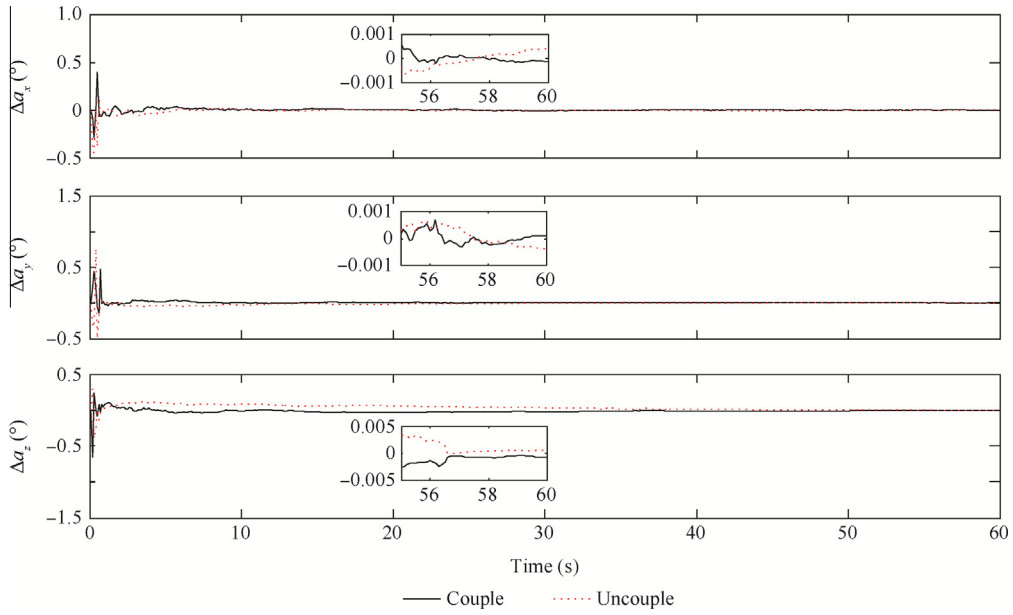

Fig. 5 Attitude estimation errors.

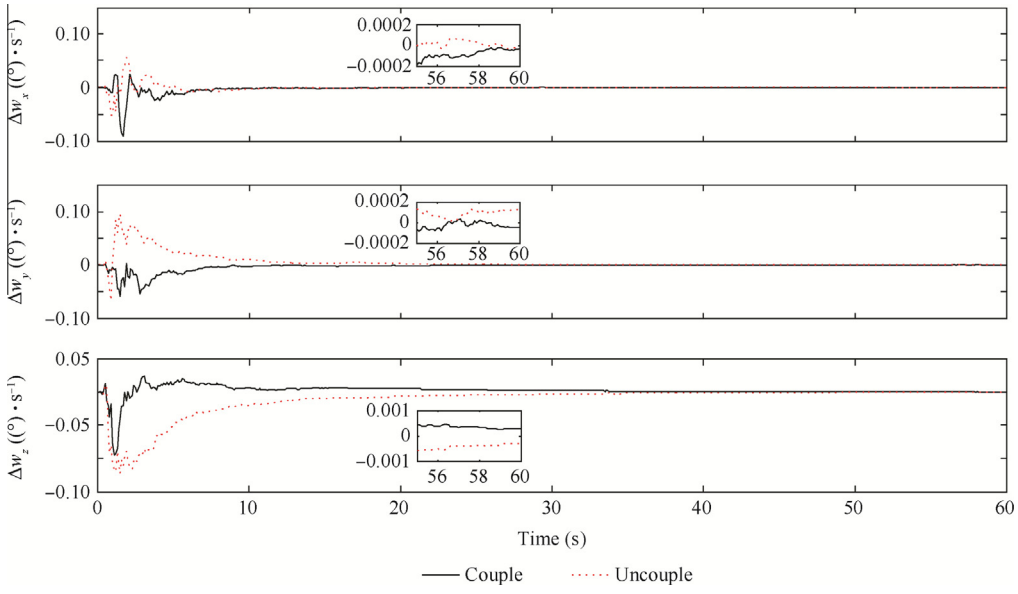

Fig. 6 Angular velocity estimation errors.

In each loop of the InCKF, it randomly takes five samples from the uniform distribution as hypotheses inertial tensor. And EKF randomly takes one sample as the target inertial tensor during the whole estimation process. Initial relative position $\boldsymbol{\rho}_0(0)$ is set as

$$\boldsymbol{\rho}_0(0) = [12.5, 12.5, 25]^{\mathrm{T}}\mathrm{m} \tag{47}$$

And the true inertial tensor of the target spacecraft and the other parameters is the same as those of example I.

Figs. 8–11 show the norm of relative states estimation errors for this example and Figs. 12–15 show the estimation errors. In addition, the norm of inertial tensor estimation

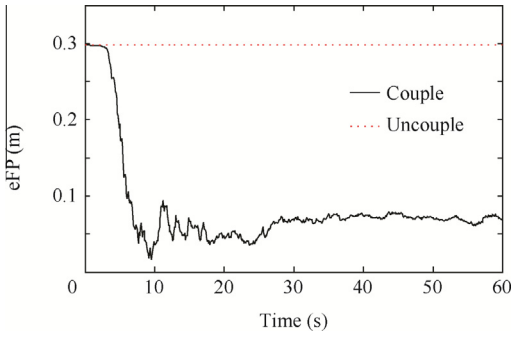

Fig. 7 Position of estimation errors of feature points.

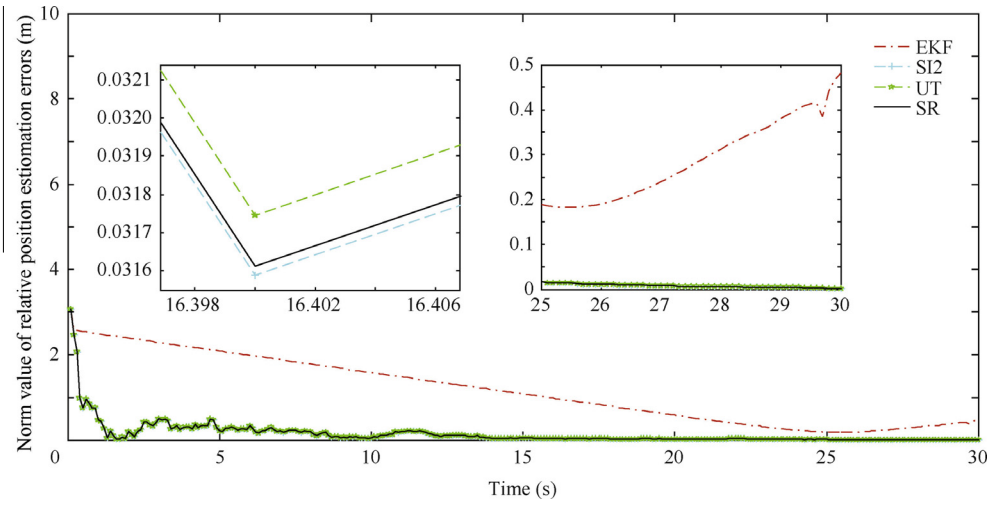

Fig. 8 Norm value of relative position estimation errors.

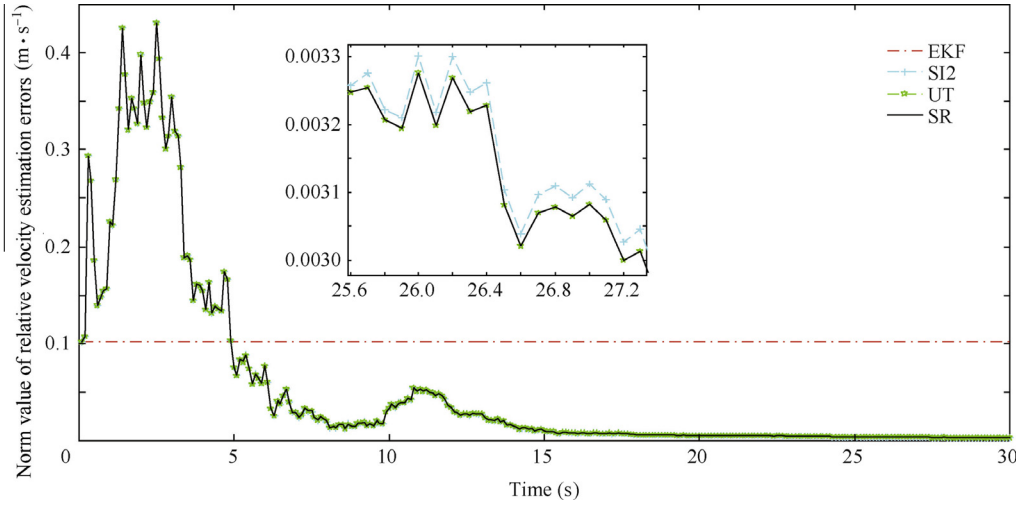

Fig. 9 Norm value of relative velocity estimation errors.

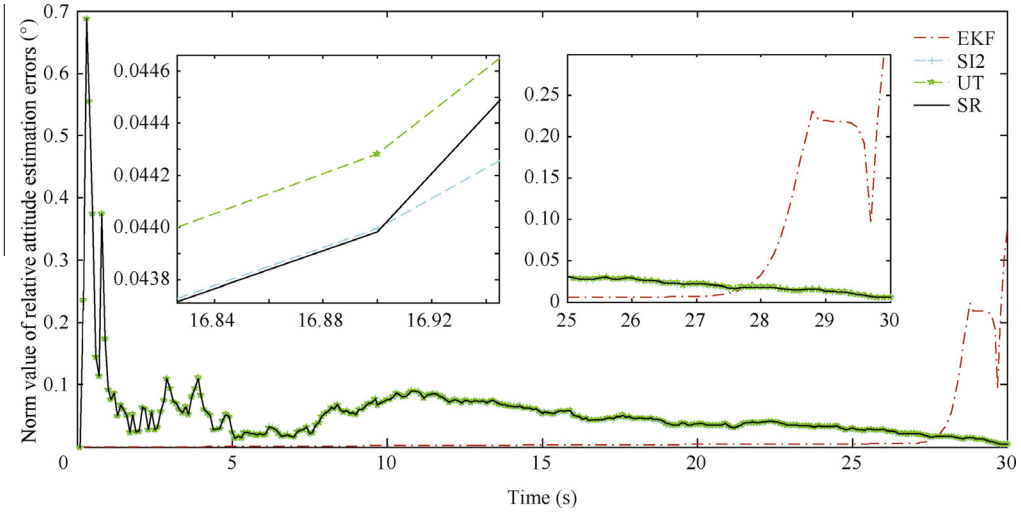

Fig. 10 Norm value of relative attitude estimation errors.

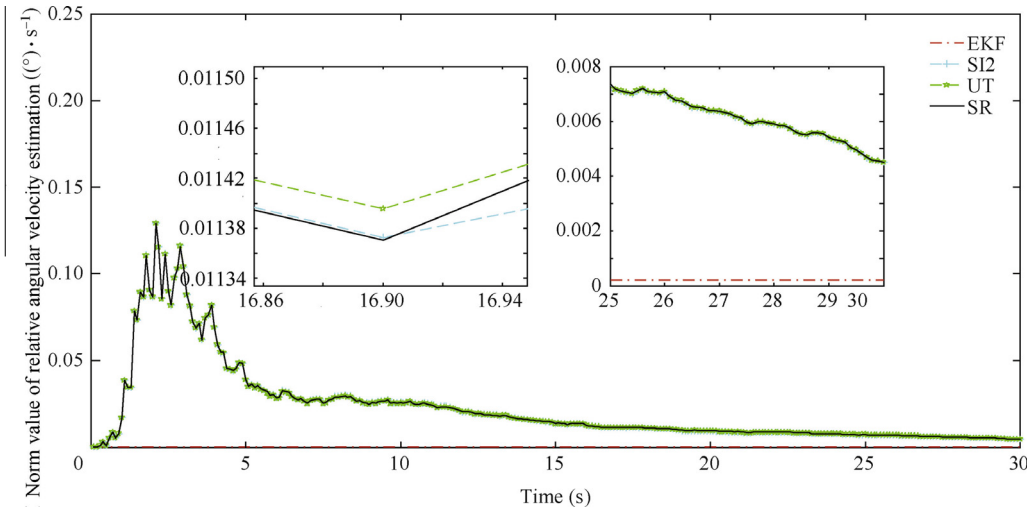

Fig. 11 Norm value of relative angular velocity estimation errors.

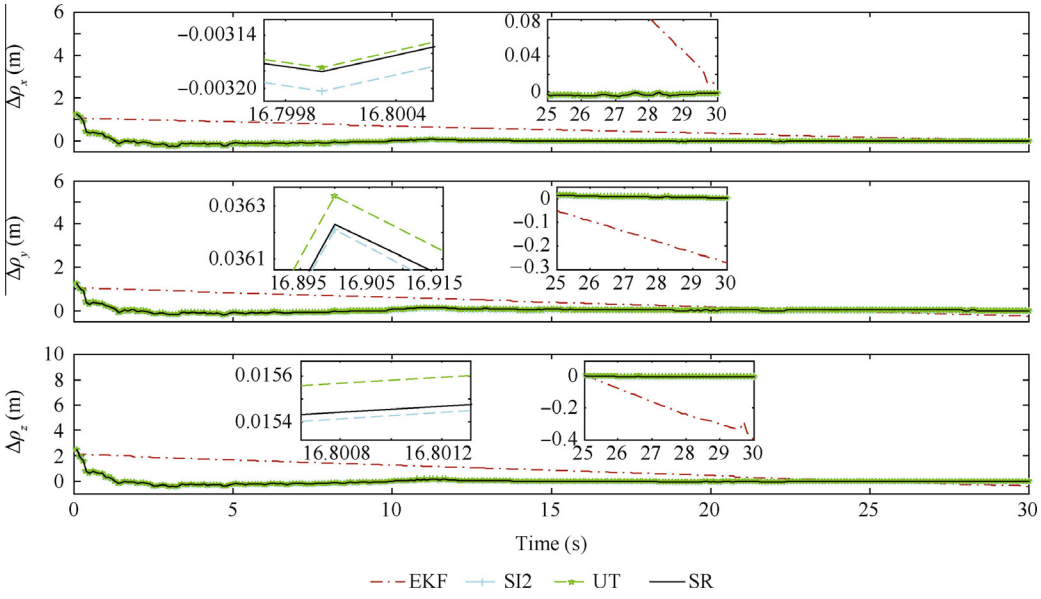

Fig. 12 Relative position estimation errors.

errors is shown in Fig. 16. In Figs. 9–11, the numerical stability of EKF with a random sampling is better than that of InCKF. However its estimation accuracy is worse than that of InCKF in Figs. 13 and 14. The difference between consecutive estimation results of EKF is small in Figs. 13 and 15, hence its corresponding norm values seem to be constant as compared with that of the InCKF. This is because that the EKF selects random sampling only once for the unknown inertial tensor in the whole estimation process, not like the multiple sampling in the InCKF, whose fluctuation of estimation results about relative velocity and relative angular velocity is small. It is implied that the uncertainty of inertial tensor effects on the estimation results is small in the case of a suitable sampling error. However, in Figs. 8, 10, 12 and 14, there is some saltation at the end of the estimation process. Especially, the results of EKF are jumped in Figs. 8 and 10 which could climb up to 0.48 m and 0.35° in a flash, respectively. And it has the trend of divergence. This is extremely dangerous for the RVD missions and it even could result in spacecraft collision. The reason for stability decline is the increase of system dimension. It cannot yield stabilized estimation for all states in the case of high-dimension system. Besides, the nonlinearity at that time is also the reason for this issue. And it implies that the original EKF without any improvement cannot manage the problem of estimation about unknown inertial tensor. Its robustness is worse than that of the InCKF.

Furthermore, it is found that the three kinds of algorithms about InCKF have the same trend and similar accuracy. In

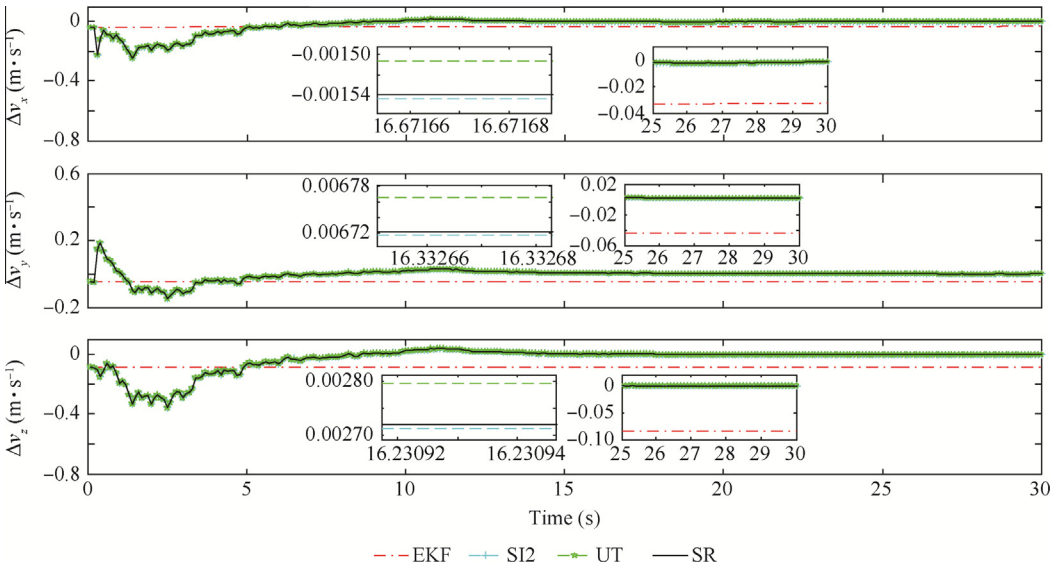

Fig. 13 Relative velocity estimation errors.

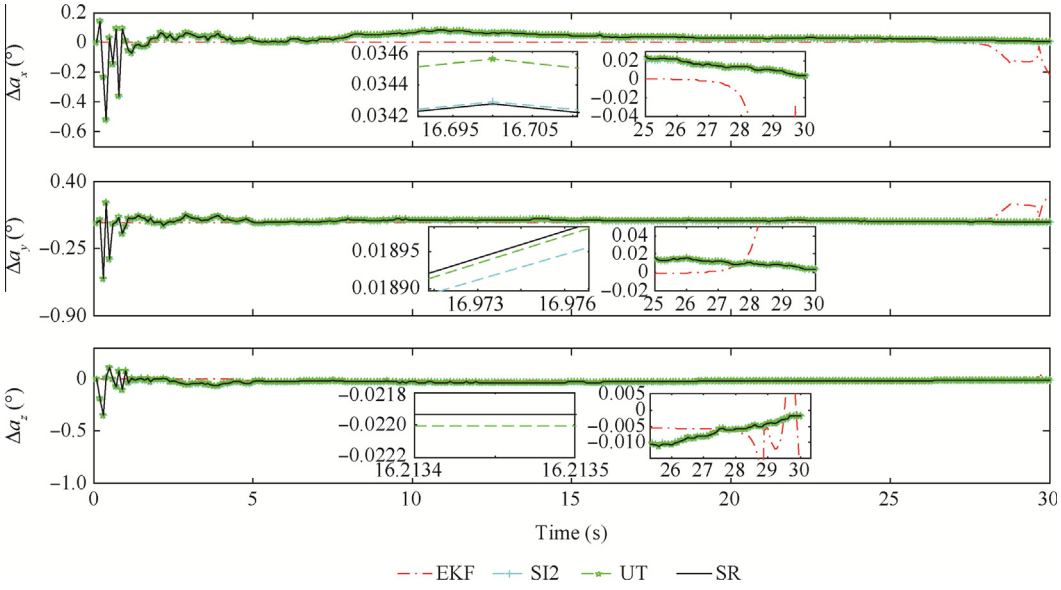

Fig. 14 Relative attitude estimation errors.

Figs. 8–15, the accuracies of the InCKF based on Stirling's interpolation and spherical-radial are a little better than those of the InCKF based on unscented transformation, and their errors are extremely small which are limited within the level of 10^{-3} in Figs. 13 and 15. This is because that the main body of InCKF algorithm is still the CKF and the states about relative position, relative velocity, relative attitude and relative angular velocity are estimated by the CKF. Their accuracy is very close and the slight difference is caused by the estimation results about inertial tensor. In Fig. 16, the inertial tensor errors of EKF are constant for it randomly samples only once. Although the inertial tensor estimation of InCKF based on Stirling's interpolation is far better than that of the InCKF based on spherical-radial and unscented transformation, the estimation results with respect to system states are similar. It is implied that the errors of inertial tensor within limits have little effect on the estimation about relative position, relative velocity, relative attitude and relative angular velocity. And the results depend largely on the nonlinear filter. In conclusion, the proposed InCKF can deal with the problems of estimation about unknown inertial tensor effectively and achieve fairly high precision.

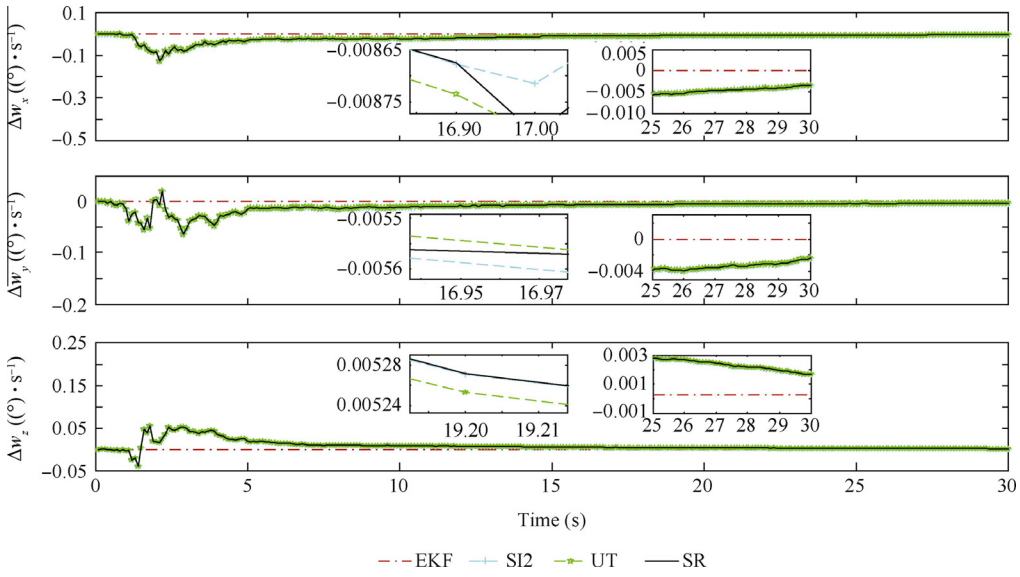

Fig. 15 Relative angular velocity estimation errors.

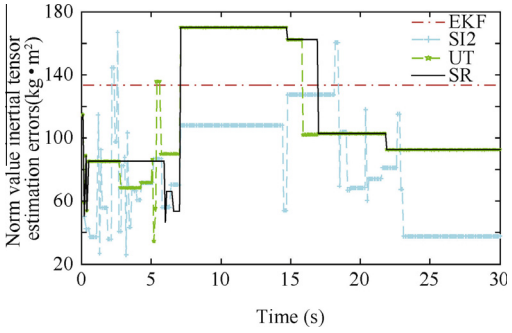

Fig. 16 Norm value of inertial tensor estimation errors.

6. Conclusions

(1) A new filter is utilized for estimating the relative states about non-cooperative spacecraft of unknown orbit elements and inertial tensor. This filter integrates a MAP estimator into multiple CKFs to identify the inertial tensor of target spacecraft. And it presents three different methods to approximate the likelihood probability with respect to the inertial tensor. Numerical simulations demonstrate that this filter is much more robust than EKF to unknown inertial tensor. In particular, the accuracy of the filter based on Stirling's interpolation and spherical-radial rule is extremely high.

(2) Furthermore, this paper presents a coupled model which incorporates kinematic couple between rotational and translational dynamics. And dynamics of the feature points is considered in this couple. Numerical simulations show that the accuracy of the couple model is much better than that of the uncouple model about estimating the position of the feature points.

(3) Different from the traditional dynamics equations which need the orbit elements of the target spacecraft, the relative dynamics in this paper is projected onto the orbital plane of the chaser spacecraft. In the case that there is not any information about the target spacecraft, it is able to satisfy the demand in RVD missions with respect to non-cooperative target well.

Acknowledgements

The authors would like to acknowledge the financial support provided by the National Natural Science Foundation of China (Nos. 61174037, 61573115), the National Basic Research Program of China (No. 2012CB821205).

References

1. Kim SG, Crassidis JL, Cheng Y, Fosbury AM, Junkins JL. Kalman filtering for relative spacecraft attitude and position estimation. *J Guid Control Dynam* 2007;**30**(1):133–43.
2. Woffinden DC, Geller DK. Navigating the road to autonomous orbital rendezvous. *J Spacecraft Rockets* 2007;**44**(4):898–909.
3. Wigbert F. *Automated rendezvous and docking of spacecraft*. New York: Cambridge University Press; 2003. p. 1–6.
4. Heaton AF, Howard RT, Pinson RM. Orbital Express AVGS validation and calibration for automated rendezvous. *Proceeding of AIAA/AAS astrodynamics specialist conference and exhibit*; 2008 Aug 18–21; Honolulu, Hawaii. Reston: AIAA. 2008. p. 1–18.
5. Kawano I, Mokuno M, Kasai T, Suzuki T. Result of autonomous rendezvous docking experiment of engineering test satellite-VII. *J Spacecraft Rockets* 2001;**38**(1):105–11.
6. Pinard D, Reynaud S, Delpy P, Strandmoe SE. Accurate and autonomous navigation for the ATV. *Aerosp Sci Technol* 2007;**11**(6):490–8.
7. Howard RT, Bryan TC. DART AVGS flight results. *Proceeding of sensors and systems for space applications*; 2007 Apr 9; Orlando, Florida, USA. Washing D.C.: SPIE; 2007. p. 1–10.
8. Zhang L, Yang H, Zhang S, Hong C, Shan Q. Kalman filtering for relative spacecraft attitude and position estimation: a revisit. *J Guid Control Dynam* 2014;**37**(5):1706–11.
9. Ambrose R, Wilcox B, Reed B, Matthies L, Lavery D, Korsmeyer D. Robotics, tele-robotics and autonomous systems roadmap technology area 04. Washington DC: National Aeronautics and Space Administration; 2010, Draft report.

10. Lanzerotti LJ. Assessment of options for extending the life of the hubble space telescope. Washington D.C.: National Academies Press; 2005, Final report.
11. Fasano G, Grassi M, Accardo D. A stereo-vision based system for autonomous navigation of an in-orbit servicing platform. *Proceeding of AIAA infotech at aerospace conference*; 2009 Apr 6–9; Seattle, Washington D.C.,USA. Reston: AIAA; 2009. p. 1–10.
12. Xu W, Liang B, Li C, Xu Y. Autonomous rendezvous and robotic capturing of non-cooperative target in space. *Robotica* 2010;**28** (5):705–18.
13. Liu H, Wang Z, Wang B, Li Z. Pose determination of non-cooperative spacecraft based on multi-feature information fusion. *Proceeding of IEEE International Conference on Robotics and Biomimetics*; 2013 Dec 12–14; Shenzhen, China. Piscataway, NJ: IEEE Press; 2013. p. 1538–43.
14. Kelsey JM, Byrne J, Cosgrove M, Seereeram S, Mehra RK. Vision-based relative pose estimation for autonomous rendezvous and docking. *Proceeding of IEEE Aerospace Conference*; Big Sky, MT. Piscataway, NJ: IEEE Prsss; 2006. p. 1–20.
15. Zhou J, Bai B, Yu X. A new method of relative position and attitude determination for non-cooperative target. *J Astronaut* 2011;**32**(3):516–21 Chinese.
16. Segal S, Gurfil P. Effect of kinematic rotation-translation coupling on relative spacecraft translational dynamics. *J Guid Control Dynam* 2009;**32**(3):1045–50.
17. Aghili F, Parsa K. Motion and parameter estimation of space objects using laser-vision data. *J Guid Control Dynam* 2009;**32** (2):537–49.
18. Zhang L, Zhang S, Yang H, Hong C, Shan Q. Relative attitude and position estimation for a tumbling spacecraft. *Aerosp Sci Technol* 2015;**42**:97–105.
19. Segal S, Carmi A, Gurfil P. Stereovision-based estimation of relative dynamics between noncooperative satellites: theory and experiments. *IEEE Trans Control Syst Technol* 2014;**22**(2):568–84.
20. Arasaratnam I, Haykin S. Cubature Kalman filters. *IEEE Trans Autom Control* 2009;**54**(6):1254–69.
21. Christopher DK, Hanspeter S. Nonsingular attitude filtering using modified Rodrigues parameters. *J Astronaut Sci* 2010;**57**(4):777–91.
22. Bay H, Ess A, Tuytelaars T, van Gool L. Speeded-up robust features (SURF). *Comput Vis Image Underst* 2008;**110**(3):346–59.
23. Crassidis JL, Junkins JL. *Optimal estimation of dynamic systems*. Boca Raton: Chapman & Hall/CRC; 2004. p. 270–82.
24. Yu H, Song S, Wang S. Interaction cubature Kalman filter and its application. Control and Decision 2015;**30** (9):1660–6 (Chinese).
25. Nrgaard M, Poulsen NK, Ravn O. New developments in state estimation for nonlinear systems. *Automatica* 2000;**36**(11): 1627–38.
26. Julier SJ, Uhlmann JK. Unscented filtering and nonlinear estimation. *Proc IEEE* 2004;**92**(3):401–22.

Yu Han received his Ph.D. degree in control science and engineering from Harbin Institute of Technology in 2015. Currently, he is an engineer at Beijing Institute of Astronautical Systems Engineering. His main research interests include vision-aided inertial navigation, nonlinear filter and effectiveness evaluation.

Zhang Xiujie received her M.S. degree in intelligence engineering from Chiba University, Chiba, Japan, in 2006. She received the Ph.D. degree in control theory and application from Harbin Institute of Technology, Harbin, China, in 2013. Her current research interests include evolutionary computation, nonlinear filter and their applications.

Liu Lingyu received his Ph.D. degree in navigation guidance and control from Beihang University in 2012. Currently, he is an engineer at Beijing Institute of Astronautical Systems Engineering. His main research interests include simulation technology and flight simulation.

Wang Shuo received his M.S. degree in control science and engineering from Heilongjiang University in 2011. Currently, he is a Ph.D. student at Harbin Institute of Technology. His main research interests include vision navigation, nonlinear filter and data fusion.

Song Shenmin received his Ph.D. degree in control theory and application from Harbin Institute of Technology in 1996. He carried out postdoctoral research at Tokyo University from 2000 to 2002. He is currently a professor at the School of Astronautics, Harbin Institute of Technology. His main research interests include spacecraft guidance and control, intelligent control, and nonlinear theory and application.